

Direct measurement of the coherent light proportion from a practical laser sourceXi Jie Yeo ¹, Eva Ernst,¹ Alvin Leow,² Jaesuk Hwang,¹ Lijiong Shen,¹ Christian Kurtsiefer ^{1,2,*} and Peng Kian Tan ¹¹*Centre for Quantum Technologies, National University of Singapore, 3 Science Drive 2, Singapore 117543*²*Department of Physics, National University of Singapore, 2 Science Drive 3, Singapore 117551*

(Received 18 October 2023; accepted 20 December 2023; published 12 January 2024)

We present a technique to estimate the proportion of coherent emission in the light emitted by a practical laser source without spectral filtering. The technique is based on measuring interferometric photon correlations between the output ports of an asymmetric Mach-Zehnder interferometer. With this, we characterize the fraction of coherent emission in the light emitted by a laser diode when transiting through the lasing threshold.

DOI: [10.1103/PhysRevA.109.013706](https://doi.org/10.1103/PhysRevA.109.013706)**I. INTRODUCTION**

The invention of lasers can be traced to work describing the emission process of the light from an atom to be spontaneous or stimulated [1]. An ensemble of atoms undergoing stimulated emission will emit coherent light that has a well-defined phase, while spontaneous emission will lead to randomly phased incoherent light [2]. Coherent light is at the core of many applications, including interferometry [3], metrology [4], and optical communication. The concepts of coherent and incoherent light also generated a fundamental interest in the statistical properties of light sources, including light sources containing a mixture of coherent and incoherent light [5–8].

In traditional models of macroscopic lasers [9–11], the emitted light is modeled to originate dominantly from stimulated emission. These models predict a phase transition of the nature of emission with increasing pump strength, separating two regimes where light emitted is either spontaneous (below threshold) or stimulated (above threshold).

However, experiments on small lasers have shown that the transition from spontaneous to stimulated emission is not abrupt [12–16]. Instead, light emitted from the laser can be described as a mixture of spontaneous and stimulated emission across a transition range.

In these experiments, the transition from spontaneous to stimulated emission was characterized by measuring the second-order photon correlation $g^{(2)}$, using a Hanbury-Brown and Twiss scheme [17]. The measurement result can be explained using Glauber’s theory of optical coherence [5], where incoherent light from spontaneous emission would exhibit a “bunching” signature with $g^{(2)}(0) > 1$, while coherent light from stimulated emission exhibits a Poissonian distribution with $g^{(2)} = 1$.

The bunching signature associated with incoherent light has a characteristic timescale inversely proportional to its spectral width according to the Wiener-Khinchine theorem [18–20]. In a practical measurement, the amplitude of the

bunching signature scales with the ratio of the characteristic timescale of the light to the timing response of the detectors [21]. Thus, when the spectral width of incoherent light is so broad that the characteristic timescale of the bunching signature is smaller than the detector timing uncertainty, incoherent light may exhibit $g^{(2)} \approx 1$, like coherent light.

To overcome the limited detector timing uncertainty, a narrow band of incoherent light can be prepared with filters from a wide optical spectrum of an incoherent light source [22]. The narrow spectral width of a filtered incoherent light has a correspondingly larger characteristic coherence timescale, which may be long enough to be resolvable by the detectors.

However, when characterizing the transition of a laser from spontaneous to stimulated emission, such spectral filtering presents some shortcomings. First, as spectral filtering discards light outside the transmission window of a filter, a result would be inconclusive for the full emission of the source. Second, spectral filtering requires *a priori* information or an educated guess of the central frequency and bandwidth of stimulated emission. Third, it has been shown that spectral filtering below the Schawlow-Townes linewidth of the laser results in $g^{(2)}(0) > 1$, similar to light from spontaneous emission [23].

Light emitted by a laser is also incoherent in multimode operation [24,25], where a laser may emit coherent light in multiple transverse and/or longitudinal modes. The light in each mode may be coherent, but a combination of multiple modes may result in a randomly phased light and therefore appear incoherent.

This motivates the search for methods for quantifying the proportion of coherent light emitted by a source without the need for spectral filtering. A method to characterize the stimulated and spontaneous emission from a pulsed laser has been demonstrated before [26,27].

In this paper, we present a method to quantify bounds for the proportion of coherent light for a continuous-wave laser. Specifically, we investigate the brightest mode of coherent emission from a semiconductor laser diode by using interferometric photon correlations, i.e., a correlation of photoevents detected at the output ports of an asymmetric Mach-Zehnder interferometer. Earlier methods of interferometric photon

*christian.kurtsiefer@gmail.com

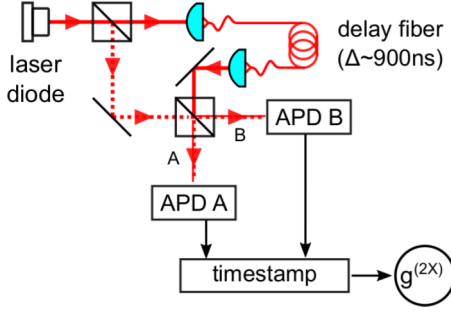


FIG. 1. Experimental setup for measuring interferometric photon correlations. Light from a laser diode enters an asymmetric Mach-Zehnder interferometer. Single-photon avalanche photodiodes (APDs) at each output port of the interferometer generate photodetection events, which are time-stamped to extract the correlations numerically.

correlation measurements were used to study spectral diffusion in organic molecules embedded in a solid matrix [28,29]. The method of interferometric photon correlation we use here was originally applied to differentiate between incoherent light and coherent light with amplitude fluctuations [30]. In contrast to second-order photon correlations, this method can clearly distinguish between finite-linewidth coherent light and broadband incoherent light through separable correlation features [31]. These separable features have characteristic time constants inversely proportional to the corresponding spectral widths of coherent and incoherent light components. The fraction of coherent light is extracted from its associated correlation feature, which decays over a characteristic timescale corresponding to the coherence time. This coherence time is typically long enough to be easily resolved by the single photodetectors with a time resolution below 1 ns. This method also allows us to obtain the spectral bandwidth of the coherent component without a spectral filter. For the incoherent component, the spectral feature is typically too wide to be detected in a time-domain photon correlation with limited detector timing resolution. Nevertheless, we can use this method to extract the fraction of coherent light emitted by the laser diode over a range of pump powers across the lasing threshold.

II. INTERFEROMETRIC PHOTON CORRELATIONS

The setup for an interferometric photon correlation measurement $g^{(2X)}$ is shown in Fig. 1. Light emitted by the laser diode is sent through an asymmetric Mach-Zehnder interferometer, with a propagation delay Δ between the two paths of the interferometer that exceeds the coherence time of the light.

With a light field $E(t)$ at the input, the light fields at the output ports A, B of the interferometer are

$$E_{A,B}(t) = \frac{E(t) \pm E(t + \Delta)}{\sqrt{2}}, \quad (1)$$

with the relative phase shift π acquired by one of the output fields from the beamsplitter.

Using these expressions for the electrical fields, the temporal correlation of photodetection events between the two

output ports is given by

$$g^{(2X)}(t_2 - t_1) = \frac{\langle E_A^*(t_1)E_B^*(t_2)E_B(t_2)E_A(t_1) \rangle}{\langle E_A^*(t_1)E_A(t_1) \rangle \langle E_B^*(t_2)E_B(t_2) \rangle}. \quad (2)$$

Here, $\langle \rangle$ indicates an expectation value and/or an ensemble average. Using Eq. (1), $g^{(2X)}(t_2 - t_1)$ can be grouped into several terms:

$$\begin{aligned} g^{(2X)}(t_2 - t_1) &= \frac{1}{4} [\langle E^*(t_1)E^*(t_2)E(t_2)E(t_1) \rangle \\ &+ \langle E^*(t_1 + \Delta)E^*(t_2 + \Delta)E(t_2 + \Delta)E(t_1 + \Delta) \rangle \\ &+ \langle E^*(t_1 + \Delta)E^*(t_2)E(t_2)E(t_1 + \Delta) \rangle \\ &+ \langle E^*(t_1)E^*(t_2 + \Delta)E(t_2 + \Delta)E(t_1) \rangle \\ &- \langle E^*(t_1 + \Delta)E^*(t_2)E(t_2 + \Delta)E(t_1) \rangle \\ &- \langle E^*(t_1)E^*(t_2 + \Delta)E(t_2)E(t_1 + \Delta) \rangle]. \end{aligned} \quad (3)$$

The first two terms have the form of conventional second-order photon correlation functions $g^{(2)}(t_2 - t_1)$. The next two terms are conventional second-order photon correlation functions, time-shifted forward and backward in their argument by the propagation delay Δ . The last two terms reduce $g^{(2X)}$, leading to a dip at zero time difference $t_2 - t_1 = 0$, with a width given by the coherence time of the light.

The expectation values appearing in Eq. (3) can be evaluated by using statistical expressions [2] of $E(t)$ for incoherent and coherent light [31].

For incoherent light, $g^{(2X)}$ exhibits a bunching signature peaking at time differences $\pm\Delta$, $g^{(2X)}(\pm\Delta) = 1 + (1/4)$. At zero time difference, the expected bunching signature from conventional second-order photon correlation functions in the first two terms and the dip from the last two terms of Eq. (3) cancel each other, resulting in $g^{(2X)}(0) = 1$.

For coherent light, the second-order photon correlation function $g^{(2)} = 1$ combines with the negative contributions from the last two terms of Eq. (3) such that $g^{(2X)}(0) = 1/2$. As these negative contributions are related to the first-order coherence of the light source, the shape of the dip can be used to obtain the spectral distribution of this light source component through a Fourier transform.

III. FRACTION OF COHERENT LIGHT IN A MIXTURE

In order to obtain an interpretation of the nature of the light emitted beyond just presenting the components of $g^{(2X)}$, we consider a light field that is neither completely coherent nor incoherent. We assume that light emitted by the laser is a mixture of a coherent light field E_{coh} and a light field E_{unc} uncorrelated to E_{coh} . The nature of E_{unc} can be coherent, incoherent, or a coherent-incoherent mixture. As E_{unc} may also be a mixture of uncorrelated coherent modes, E_{coh} here represents the coherent mode in the mixture with the highest intensity. In the following, we extract quantitative information about the components of the light field from interferometric photon correlations $g^{(2X)}$, namely the fraction of optical power in the brightest coherent component.

We model the light field mixture with an electrical field

$$E_{\text{mix}}(t) = \sqrt{\rho}E_{\text{coh}}(t) + \sqrt{1 - \rho}E_{\text{unc}}(t), \quad (4)$$

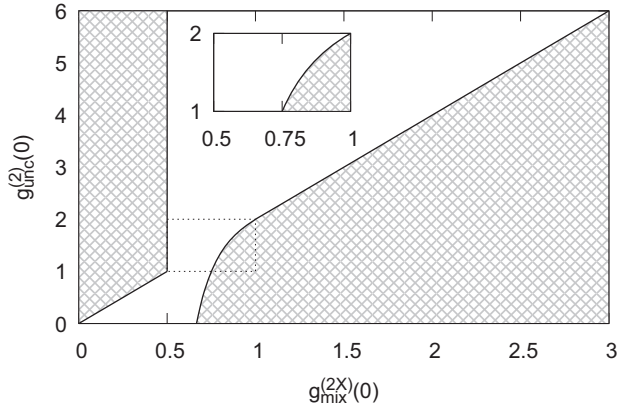


FIG. 2. Combinations of $g_{\text{unc}}^{(2)}(0)$ and $g_{\text{mix}}^{(2X)}(0)$ that correspond to physical and real-valued ρ . In shaded areas, no such solution exist. Inset: Zoom into the region $1 \leq g_{\text{unc}}^{(2)}(0) \leq 2$, where the uncorrelated light source is assumed to be a mixture of coherent and completely incoherent light and thermal light.

where ρ is the fraction of optical power of the brightest coherent emission and the respective light field terms are normalized such that $|E_{\text{mix}}| = |E_{\text{coh}}| = |E_{\text{unc}}|$.

Evaluating photon correlation in Eq. (3) with this light model and further assuming that first, the propagation delay in the interferometer is significantly longer than the coherence timescale of the light source and, second, the interferometer has good visibility yields

$$g_{\text{mix}}^{(2X)}(0) = 2\rho - \frac{3\rho^2}{2} + \frac{(1-\rho)^2}{2} g_{\text{unc}}^{(2)}(0) \quad (5)$$

at zero time difference, with only two remaining parameters, ρ and $g_{\text{unc}}^{(2)}(0)$, the second-order photon correlation of the uncorrelated field at zero time difference (see Appendix A).

The connection in Eq. (5), together with the physical requirement $0 \leq \rho \leq 1$ for the fraction of coherent light, limits the possible combinations of $g_{\text{unc}}^{(2)}(0)$ and $g_{\text{mix}}^{(2X)}(0)$, shown as nonshaded areas in Fig. 2; the exact expressions for the boundaries are given in Appendix B.

We can now further assume that the uncorrelated light source generates some mixture of coherent and completely incoherent light [$g^{(2)}(0) = 1$] and thermal light [$g^{(2)}(0) = 2$]. This constrains the second-order photon correlation of the uncorrelated light:

$$1 \leq g_{\text{unc}}^{(2)}(0) \leq 2. \quad (6)$$

We impose these bounds in Eq. (5) and extract the bounds to the fraction of optical power in the brightest coherent emission ρ with an upper bound,

$$\rho \leq \sqrt{2 - 2g_{\text{mix}}^{(2X)}(0)}, \quad (7)$$

and a lower bound,

$$\rho \geq \begin{cases} \frac{1}{2} + \frac{1}{2}\sqrt{3 - 4g_{\text{mix}}^{(2X)}(0)} & \text{for } \frac{1}{2} \leq g_{\text{mix}}^{(2X)}(0) \leq \frac{3}{4} \\ 2 - 2g_{\text{mix}}^{(2X)}(0) & \text{for } \frac{3}{4} \leq g_{\text{mix}}^{(2X)}(0) \leq 1, \end{cases} \quad (8)$$

with $g_{\text{mix}}^{(2X)}(0)$ ranging from 1/2 for fully coherent light to 1 for fully incoherent light.

In practice, these two bounds for ρ are quite tight and allow us to extract the fraction ρ in an experiment with a small uncertainty.

IV. EXPERIMENT

In our experiment, we measure interferometric photon correlations of light emitted from a temperature-stabilized distributed feedback laser diode with a central wavelength around 780 nm.

The setup is shown in Fig. 1. Interferometric photon correlations are obtained from an asymmetric Mach-Zehnder interferometer, formed by 50 : 50 fiber beamsplitters and a propagation delay Δ of about 900 ns through a 180-m-long single-mode optical fiber in one of the arms. Photoevents at each output port of the interferometer were detected with actively quenched silicon single-photon avalanche photodiodes (APDs). The detected photoevents were time-stamped with a resolution of 2 ns for an integration time T .

The correlation function $g^{(2X)}$ is extracted by drawing a histogram of all time differences $t_2 - t_1$ between detection event pairs in the interval T numerically, which allows for a clean normalization.

The shape of the dip in $g^{(2X)}$ is related to the spectral line shape of the coherent light through a Fourier transform. If we assume that the coherent light emitted by a laser has a Lorentzian line shape [32], the resulting correlation can be modeled by a two-sided exponential function,

$$g^{(2X)}(t_2 - t_1) = 1 - A \cdot \exp\left(-\frac{|t_2 - t_1|}{\tau_c}\right), \quad (9)$$

where τ_c is the characteristic time constant of the coherent light and A is the amplitude of the dip. The value of $g^{(2X)}(0)$ is extracted from the fit as $1 - A$. Examples of measured correlation functions and corresponding fits for different laser powers are shown in Fig. 3.

A. Transition from incoherent to coherent light

A transition from incoherent to coherent emission is expected as the laser current is increased across the lasing threshold of the laser. We identify the lasing threshold of a laser diode I_T by measuring the steepest increase of optical power with the laser current (Fig. 4). For our diode, we find $I_T = 37$ mA.

To observe the transition from incoherent to coherent emission, we extract the fraction ρ of optical power in the brightest coherent component in the light field at different values of the laser current I_L across the lasing threshold from measurements of $g^{(2X)}$ (Fig. 5, top panel). The amplitude of the dip is extracted by fitting these correlations to Eq. (9), from which the upper bound and lower bound of ρ are extracted (Fig. 5, middle panel).

From the fit, ρ remains near 0 below threshold. Above the threshold, ρ increases quickly with I_L in a phase-transition manner, reaching $\rho = 0.986$ (90% confidence interval, 0.982–0.989) at $I_L = 120$ mA. This agrees with the expectation that the emission of the laser diode is increasingly dominated by stimulated emission when driven with current above the lasing threshold [33,34].

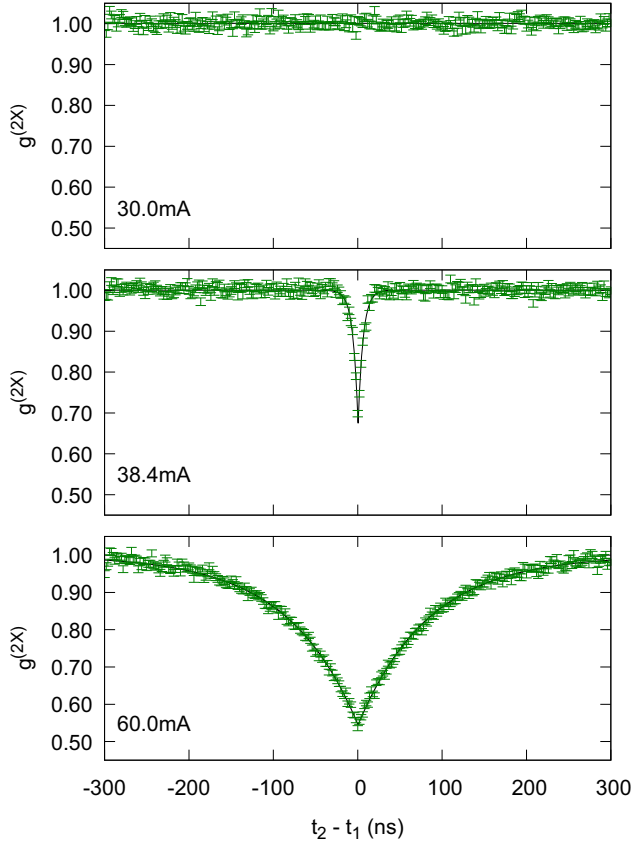


FIG. 3. Interferometric photon correlations $g^{(2X)}$ for different laser currents I_L , extracted from a histogram of photodetector time differences (green symbols). The error range at a specific time bin indicates an expected uncertainty according to Poissonian counting statistics. The black solid curves show a fit to Eq. (9), resulting in values for A (from top to bottom) of -0.0006 ± 0.0003 , 0.326 ± 0.008 , and 0.455 ± 0.002 , respectively.

The upper and lower bounds for ρ from Eqs. (7) and (8) are quite tight even near the lasing threshold, suggesting that the mixture model equation (4) captures the nature of the light through the phase transition well.

The coherence time of the coherent light τ_c can also be extracted by fitting $g^{(2X)}$ measurements to Eq. (9) (Fig. 5, bottom

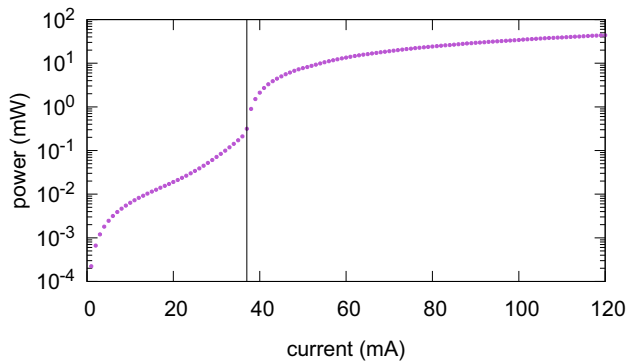


FIG. 4. Measured laser power against laser current I_L . The sharpest change is observed at $I_T = 37$ mA, indicating the threshold current (dashed line).

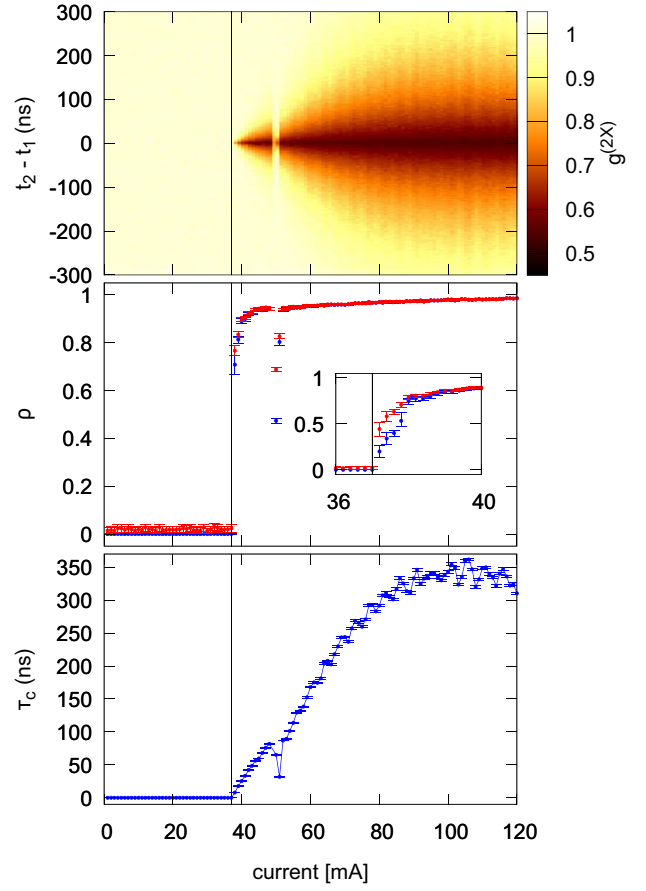


FIG. 5. Top: Interferometric photon correlations $g^{(2X)}$ for different laser currents I_L . Middle: Corresponding upper bound of fraction ρ of coherent light (red) extracted via Eq. (C1), and the lower bound (blue) extracted via Eq. (C2) from $g^{(2X)}(0)$. The dip in ρ is a result of emission at multiple chip modes as explained in Sec. IV B. The inset shows the extracted bounds for ρ at finer steps of laser current near the lasing threshold. Bottom: Coherence time of coherent light τ_c extracted from $g^{(2X)}$. The dashed line indicates the threshold current $I_T = 37$ mA.

panel). We observe that the coherence time increases with the current after the threshold current, before reaching a steady value between 300 and 350 ns. The increase of coherence time corresponds to a narrowing of the emission linewidth. This observation agrees with predictions from laser theory that line narrowing is expected with increased pumping [34]. A small modulation of the coherence time becomes visible for larger laser currents, with a periodicity of about 6 mA.

B. Light statistics near a mode hop

Above the threshold, the laser can oscillate at different longitudinal modes for different laser currents. It is interesting to observe the presented method for extracting the fraction of coherent emission near such a mode hop, where two coherent emission modes compete.

For this, the spectrum of light emitted by the laser diode was recorded at different laser currents with an optical spectrum analyzer with a spectral resolution of 2 GHz (Bristol 771B-NIR). The laser diode emitted light into two distinct

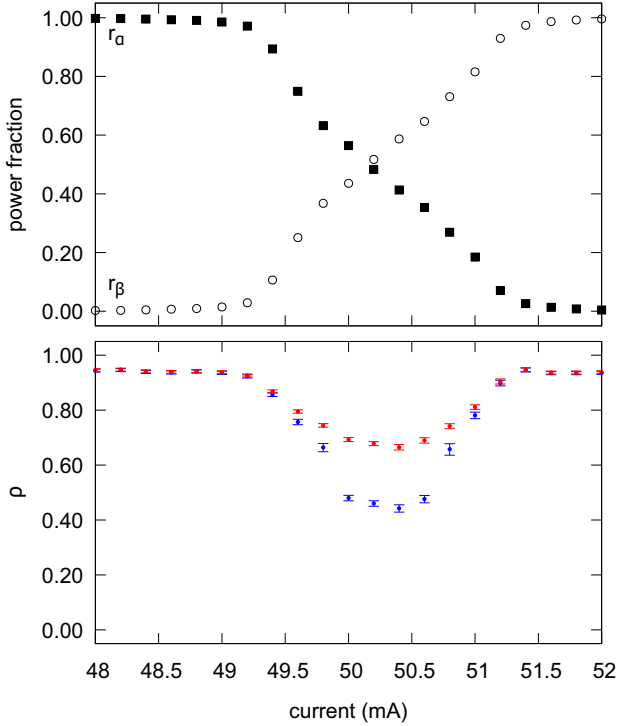


FIG. 6. Different chip modes of the laser diode are excited for different currents, resulting in a reduction of the $g^{(2X)}$ signature in a mode competition regime. Top: Power ratios $r_{\alpha,\beta}$ as a function of current for the chip modes α and β around 780.07 nm (solid squares) and 780.34 nm (open circles), respectively. Bottom: Upper bound of the fraction ρ of coherent light (red) extracted via Eq. (C1), and the lower bound (blue) extracted via Eq. (C2) from $g^{(2X)}(0)$.

narrow spectral bands with a changing power ratio in the laser current range between 49 and 52 mA. Outside this window, only one of the modes could be identified. Below 49 mA, the laser emission was centered around 780.07 nm, and above 52 mA it was centered around 780.34 nm.

The power fractions $r_{\alpha,\beta}$ of these two chip modes α and β near the mode hop,

$$r_{\alpha,\beta} = \frac{P_{\alpha,\beta}}{P_\alpha + P_\beta}, \quad (10)$$

undergo a nearly linear transition (Fig. 6, top panel).

We measured $g^{(2X)}$ in the same transition regime and extract ρ as described above (Fig. 6, bottom panel). In the transition regime, ρ decreases when both chip modes are present. This can be interpreted as coherent light in one emission band being uncorrelated to coherent light in the other one, but we did not carry out a measurement that would test for a phase relationship between the two modes.

V. CONCLUSION

We presented a method to extract the fraction of coherent light in the emission of a laser by using interferometric photon correlations. As a demonstration, we analyzed light emitted from a diode laser over a range of laser currents and observe a continuously increasing fraction of coherent light with increasing laser current above the lasing

threshold. Applying this technique to light emitted near a mode hop between longitudinal modes suggests a reduction of the fraction of coherent light in the transition regime and an interpretation that the two longitudinal modes can be viewed as mutually incoherent coherent emissions. Apart from the characterization of lasers, this method can be useful in practical applications of continuous-variable quantum key distribution protocols, where the noise of lasers as a source of coherent states needs to be carefully characterized to ensure security claims [35–37].

ACKNOWLEDGMENTS

We acknowledge support of this work by the Ministry of Education in Singapore and the National Research Foundation, Prime Minister's office, through the Research Centres of Excellence program.

APPENDIX A: INTERFEROMETRIC PHOTON CORRELATION FOR A MIXTURE OF LIGHT FIELDS

The evaluation of $g^{(2X)}$ via Eq. (3) requires the conventional second-order photon correlation function $g^{(2)}(t_1 - t_2) = \langle E^*(t_1)E^*(t_2)E(t_2)E(t_1) \rangle$. For the light field mixture equation (4), this is

$$\begin{aligned} g_{\text{mix}}^{(2)}(t_2 - t_1) &= \rho^2 g_{\text{coh}}^{(2)}(t_2 - t_1) + (1 - \rho)^2 g_{\text{unc}}^{(2)}(t_2 - t_1) \\ &\quad + 2\rho(1 - \rho)(1 + \text{Re}[g_{\text{coh}}^{(1)}(t_2 - t_1)g_{\text{unc}}^{(1)*}(t_2 - t_1)]), \end{aligned} \quad (A1)$$

where $g^{(1)}$ is the first-order field correlation function for the respective component light fields, $g^{(1)*}$ is its complex conjugate, and $\text{Re}[\dots]$ extracts the real part of its argument.

The last term in Eq. (3) can be written as

$$\begin{aligned} \langle E_{\text{mix}}^*(t_1)E_{\text{mix}}^*(t_2 + \Delta)E_{\text{mix}}(t_2)E_{\text{mix}}(t_1 + \Delta) \rangle &= \rho^2 |g_{\text{coh}}^{(1)}(t_2 - t_1)|^2 + (1 - \rho)^2 |g_{\text{unc}}^{(1)}(t_2 - t_1)|^2 \\ &\quad + 2\rho(1 - \rho) \text{Re}[g_{\text{coh}}^{(1)}(t_2 - t_1)g_{\text{unc}}^{(1)*}(t_2 - t_1)] \\ &\quad + 2\rho(1 - \rho) \text{Re}[g_{\text{coh}}^{(1)}(\Delta)g_{\text{unc}}^{(1)*}(\Delta)], \end{aligned} \quad (A2)$$

where $g^{(1)}(\Delta) \approx 0$ for our experimental situation of the propagation delay Δ being significantly larger than the coherence times of the respective light sources. Note that all terms in Eq. (A2) are real valued.

With this, the interferometric photon correlation at zero time difference in Eq. (3) is given by

$$\begin{aligned} g_{\text{mix}}^{(2X)}(0) &= \frac{1}{4}[g_{\text{mix}}^{(2)}(\Delta) + g_{\text{mix}}^{(2)}(-\Delta) \\ &\quad + 2(\rho^2 g_{\text{coh}}^{(2)}(0) + (1 - \rho)^2 g_{\text{unc}}^{(2)}(0) + 2\rho(1 - \rho)) \\ &\quad - 2(\rho^2 |g_{\text{coh}}^{(1)}(0)|^2 + (1 - \rho)^2 |g_{\text{unc}}^{(1)}(0)|^2)]. \end{aligned} \quad (A3)$$

We further assume that (1) the propagation delay in the interferometer Δ is significantly longer than the coherence timescale of the light source, such that $g_{\text{mix}}^{(2)}(\pm\Delta) \approx 1$, (2) the interferometer has high visibility such that $|g^{(1)}(0)| \approx 1$,

and (3) the second-order correlation of the coherent light field is $g_{\text{coh}}^{(2)}(0) = 1$. With this, Eq. (A3) leads to the relationship shown in Eq. (5).

APPENDIX B: BOUNDARIES OF PHYSICALLY MEANINGFUL COMBINATIONS OF INTERFEROMETRIC CORRELATIONS IN A MIXTURE

Assuming a binary mixture of the light field as per Eq. (4), the interferometric correlation of the mixture, $g_{\text{mix}}^{(2X)}(0)$, and the conventional second-order correlation of the incoherent light, $g_{\text{unc}}^{(2)}(0)$, at zero time difference are constrained by relation equation (5). Further assuming the physical requirement $0 \leq \rho \leq 1$ for the fraction ρ gives a lower bound for $g_{\text{unc}}^{(2)}(0)$,

$$g_{\text{unc}}^{(2)}(0) \geq \begin{cases} 0, & g_{\text{mix}}^{(2X)}(0) \leq \frac{2}{3} \\ 3 + \frac{1}{1-2g_{\text{mix}}^{(2X)}(0)}, & g_{\text{mix}}^{(2X)}(0) \in [\frac{2}{3}, 1] \\ 2g_{\text{mix}}^{(2X)}(0), & g_{\text{mix}}^{(2X)}(0) \geq 1. \end{cases} \quad (\text{B1})$$

For $g_{\text{mix}}^{(2X)}(0) \in [0, \frac{1}{2})$, there is an upper bound

$$g_{\text{unc}}^{(2)}(0) \leq 2g_{\text{mix}}^{(2X)}(0). \quad (\text{B2})$$

APPENDIX C: ERROR PROPAGATION FROM FITTING OF $g^{(2X)}$ MEASUREMENT

Standard error propagation techniques of experimental data through Eqs. (7)–(9) lead to infinite uncertainties for some dip amplitudes A and are therefore not used. Instead, we extract upper and lower bounds of ρ . Equation (7) provides an upper bound

$$\rho \leq \sqrt{2A}, \quad (\text{C1})$$

and Eq. (8) provides the lower bound

$$\rho \geq \begin{cases} 2A & \text{for } 0 \leq A \leq \frac{1}{4} \\ \frac{1}{2} + \frac{1}{2}\sqrt{4A-1} & \text{for } \frac{1}{4} \leq A \leq \frac{1}{2} \end{cases} \quad (\text{C2})$$

for ρ . The probability density for values of A in a measured ensemble is assumed to be a normal distribution, with a mean value and standard deviation extracted from the fit of measured $g^{(2X)}$ to Eq. (9). This can be transformed into a probability distribution for upper and lower bounds for ρ using Eqs. (C1) and (C2). We exclude nonphysical values of ρ outside $0 \leq \rho \leq 1$ and renormalize the resulting distribution to compute an expectation value of ρ and a 90% confidence interval shown in Fig. 6.

-
- [1] A. Einstein, Strahlungs-Emission und -Absorption nach der Quantentheorie, *Verh. Dtsch. Phys. Ges.* **18**, 318 (1916).
- [2] R. Loudon, *The Quantum Theory of Light* (Oxford University Press, Oxford, UK, 2000).
- [3] P. Hariharan, *Basics of Interferometry* (Elsevier, Amsterdam, 2007).
- [4] D. L. Wright, Laser metrology, in *Developments in Laser Technology I*, Proceedings of SPIE Vol. 0020 (SPIE, Bellingham, WA, 1969).
- [5] R. J. Glauber, The quantum theory of optical coherence, *Phys. Rev.* **130**, 2529 (1963).
- [6] G. Lachs, Theoretical aspects of mixtures of thermal and coherent radiation, *Phys. Rev.* **138**, B1012 (1965).
- [7] H. Morawitz, Coherence properties and photon correlation, *Phys. Rev.* **139**, A1072 (1965).
- [8] E. Jakeman and E. R. Pike, Statistics of heterodyne detection of Gaussian light, *J. Phys. A: Math. Gen.* **2**, 115 (1968).
- [9] W. E. Lamb, Theory of an optical maser, *Phys. Rev.* **134**, A1429 (1964).
- [10] F. Arecchi and R. Bonifacio, Theory of optical maser amplifiers, *IEEE J. Quantum Electron.* **1**, 169 (1965).
- [11] H. Haken, Cooperative phenomena in systems far from thermal equilibrium and in nonphysical systems, *Rev. Mod. Phys.* **47**, 67 (1975).
- [12] Y.-S. Choi, M. T. Rakher, K. Hennessy, S. Strauf, A. Badolato, P. M. Petroff, D. Bouwmeester, and E. L. Hu, Evolution of the onset of coherence in a family of photonic crystal nanolasers, *Appl. Phys. Lett.* **91**, 031108 (2007).
- [13] S. M. Ulrich, C. Gies, S. Ates, J. Wiersig, S. Reitzenstein, C. Hofmann, A. Löffler, A. Forchel, F. Jahnke, and P. Michler, Photon statistics of semiconductor microcavity lasers, *Phys. Rev. Lett.* **98**, 043906 (2007).
- [14] J. Wiersig, C. Gies, F. Jahnke, M. Aßmann, T. Berstermann, M. Bayer, C. Kistner, S. Reitzenstein, C. Schneider, S. Höfling, A. Forchel, C. Kruse, J. Kalden, and D. Hommel, Direct observation of correlations between individual photon emission events of a microcavity laser, *Nature (London)* **460**, 245 (2009).
- [15] R. Hosten, R. Braive, L. L. Gratiet, A. Talneau, G. Beaudoin, I. Robert-Philip, I. Sagnes, and A. Beveratos, Demonstration of coherent emission from high- β photonic crystal nanolasers at room temperature, *Opt. Lett.* **35**, 1154 (2010).
- [16] S. Kreinberg, W. W. Chow, J. Wolters, C. Schneider, C. Gies, F. Jahnke, S. Höfling, M. Kamp, and S. Reitzenstein, Emission from quantum-dot high- β microcavities: Transition from spontaneous emission to lasing and the effects of superradiant emitter coupling, *Light Sci. Appl.* **6**, e17030 (2017).
- [17] R. Hanbury-Brown and R. Q. Twiss, Correlation between photons in two coherent beams of light, *Nature (London)* **177**, 27 (1956).
- [18] N. Wiener, Generalized harmonic analysis, *Acta Math.* **55**, 117 (1930).
- [19] A. Khintchine, Korrelationstheorie der stationären stochastischen Prozesse, *Math. Ann.* **109**, 604 (1934).
- [20] L. Mandel and E. Wolf, *Optical Coherence and Quantum Optics* (Cambridge University Press, Cambridge U.K., 1995).
- [21] D. B. Scarf, Measurements of photon correlations in partially coherent light, *Phys. Rev.* **175**, 1661 (1968).
- [22] P. K. Tan and C. Kurtsiefer, Temporal intensity interferometry for characterization of very narrow spectral lines, *Mon. Not. R. Astron. Soc.* **469**, 1617 (2017).
- [23] R. Centeno Neelen, D. M. Boersma, M. P. van Exter, G. Nienhuis, and J. P. Woerdman, Spectral filtering within the Schawlow-Townes linewidth of a semiconductor laser, *Phys. Rev. Lett.* **69**, 593 (1992).
- [24] H. P. Weber and H. G. Danielmeyer, Multimode effects in intensity correlation measurements, *Phys. Rev. A* **2**, 2074 (1970).
- [25] J. Yin, S. Zhu, W. Gao, and Y. Wang, Second-order coherence $g^{(2)}(\tau)$ and its frequency-dependent characteristics

- of a two-longitudinal-mode laser, *Appl. Phys. B* **64**, 65 (1996).
- [26] M. Aßmann, F. Veit, M. Bayer, C. Gies, F. Jahnke, S. Reitzenstein, S. Höfling, L. Worschech, and A. Forchel, Ultrafast tracking of second-order photon correlations in the emission of quantum-dot microresonator lasers, *Phys. Rev. B* **81**, 165314 (2010).
- [27] A. George, A. Bruhacs, A. Aadhi, W. E. Hayenga, R. Ostic, E. Whitby, M. Kues, Z. M. Wang, C. Reimer, M. Khajavikhan, and R. Morandotti, Time-resolved second-order coherence characterization of broadband metallic nanolasers, *Laser Photonics Rev.* **15**, 2000593 (2021).
- [28] X. Brokmann, M. Bawendi, L. Coolen, and J.-P. Hermier, Photon-correlation Fourier spectroscopy, *Opt. Express* **14**, 6333 (2006).
- [29] L. Coolen, X. Brokmann, and J.-P. Hermier, Modeling coherence measurements on a spectrally diffusing single-photon emitter, *Phys. Rev. A* **76**, 033824 (2007).
- [30] A. Lebreton, I. Abram, R. Braive, I. Sagnes, I. Robert-Philip, and A. Beveratos, Unequivocal differentiation of coherent and chaotic light through interferometric photon correlation measurements, *Phys. Rev. Lett.* **110**, 163603 (2013).
- [31] A. Lebreton, I. Abram, R. Braive, I. Sagnes, I. Robert-Philip, and A. Beveratos, Theory of interferometric photon-correlation measurements: Differentiating coherent from chaotic light, *Phys. Rev. A* **88**, 013801 (2013).
- [32] A. Siegman, *Lasers* (University Science Books, Mill Valley, CA, 1986).
- [33] H. Haug and H. Haken, Theory of noise in semiconductor laser emission, *Z. Phys. A* **204**, 262 (1967).
- [34] H. Haken, *Light: Laser Light Dynamics* (North-Holland, Amsterdam, 1981).
- [35] Y. Shen, J. Yang, and H. Guo, Security bound of continuous-variable quantum key distribution with noisy coherent states and channel, *J. Phys. B: At., Mol. Opt. Phys.* **42**, 235506 (2009).
- [36] V. C. Usenko and R. Filip, Feasibility of continuous-variable quantum key distribution with noisy coherent states, *Phys. Rev. A* **81**, 022318 (2010).
- [37] Y. Shen, X. Peng, J. Yang, and H. Guo, Continuous-variable quantum key distribution with Gaussian source noise, *Phys. Rev. A* **83**, 052304 (2011).